Adsorption (2006) 12:227–235
DOI 10.1007/s10450-006-0142-3

Natural gas storage cycles: Influence of nonisothermal effects and heavy alkanes

Krista S. Walton · M. Douglas LeVan

Received: 23 March 2005 / Revised: 22 November 2005 / Accepted: 6 March 2006

Abstract A mathematical model is developed for examining the influence of nonisothermal effects and accumulation of heavy alkanes on natural gas storage cycles. The model is solved for the charge and discharge steps of the cycle. This is the first study to solve the natural gas storage problem for a nonisothermal charge of natural gas containing impurities. We examine both adiabatic and isothermal operation of natural gas and pure methane storage cycles on BPL carbon and an activated carbon prepared from coconut shells. Our simulations show for both carbons that the adiabatic gas storage cycles operate under subcooled conditions with respect to the feed temperature due to long discharge times and the desorption heat. It is also shown that degradation of gas storage performance due to impurities depends more on selectivity of the material for heavy alkanes than on adsorption capacities.

Keywords Natural gas storage · Simulation · Multicomponent

1 Introduction

Natural gas (NG) as a vehicular fuel has many advantages over gasoline and diesel. It is relatively abundant and clean burning, producing less hydrocarbons, NO_x, and SO_x than the other fuels. Natural gas vehicles (NGVs) are a proven technology, and there are currently more than one million in operation worldwide (Yang, 2003).

In general, NGVs compete effectively with gasoline vehicles in functionality and performance, but problems exist with onboard storage capabilities. The majority of existing NGVs operate with compressed natural gas systems (CNG). These systems typically run at high pressures (200 bar), requiring large reservoirs of compressed gas that are both expensive and unsafe.

The development of adsorbed natural gas systems (ANG) is considered to be the most promising solution for increasing storage density such that vehicles could operate at lower pressures while maintaining the same capacities as CNG (Chang and Talu, 1996). However, there are several well known problems with these types of systems that continue to impede successful commercialization. One problem can arise simply from the shape of the adsorption isotherm. ANG that utilizes an adsorbent that is characterized by a strongly concave downward or rectangular isotherm will lead to a significant loss in storage capacity because there will always be a considerable amount of natural gas adsorbed at the lower working pressure. Also, the exothermic nature of physical adsorption has a negative impact on charge and discharge in a gas storage cycle. As NG is fed to the storage vessel, the heat released during adsorption will increase the temperature of the adsorbent thereby lowering the total amount of NG that can be stored. The

Krista S. Walton · M. Douglas LeVan (✉)
Department of Chemical Engineering, Vanderbilt University, Nashville, TN 37235, USA
e-mail: m.douglas.levan@vanderbilt.edu

vessel will cool during the discharge step, decreasing the amount of NG that can be delivered.

Numerous studies of adsorptive storage systems for methane have shown that the storage container will undergo a significant temperature rise during a fast charge step and a significant decrease in temperature during discharge (Chang and Talu, 1996; Mota et al., 1995; Wegrzyn, 1996; Mota, 1997; Biloé, 2002; Zhou, 1997; Biloé et al., 2001). Slower charges, such as fueling a fleet of buses overnight, could alleviate the temperature effects for this step (Mota, 1999). However, a fast charge step seems more practical for personal vehicular use. The studies of methane discharge have shown that nonisothermal effects are important and unavoidable, even for different operating conditions (e.g., slow discharge) (Chang and Talu, 1996).

All of the studies cited thus far pertain to pure methane systems only. Storage efficiency can also be hampered by trace impurities such as higher molecular weight alkanes in the NG stream; adsorbents are typically much more selective for higher alkanes over methane. This poses a major problem for gas storage systems because the impurities can accumulate in the bed and decrease capacity for methane as the system is cycled with charge and discharge steps.

Mota (1999) developed a mathematical model for studying the cyclic behavior of an impure natural gas storage process with a feed containing the alkanes methane through pentane plus nitrogen. This is one of the only studies to consider the impact of impurities on ANG systems. Material and energy balances were solved for the discharge step, but the charge step was considered to be isothermal and perfectly mixed. Because of this latter assumption, the concentration profiles were smeared before each discharge step.

The purpose of this work is to study the effect of trace gases and nonisothermal behavior on the performance of a natural gas storage process. The mathematical model we develop is solved for full cycle concentration profiles for all components over bed length. This is the first study to treat both charge and discharge steps. We are concerned primarily with exploring the extremes of gas storage cycle behavior. From the standpoint of heat exchange of the storage vessel with the environment, the two extremes are isothermal operation, in which energies associated with adsorption and desorption would be transferred quickly through the vessel wall by heat exchange, and adiabatic operation, in which energy is transferred only through the charge and discharge gas flow. Real operation would occur somewhere between these extremes, and a large number of scenarios can be envisioned. So, we solve our model for four cases: adiabatic/methane, isothermal/methane, adiabatic/natural gas, and isothermal/natural gas. We perform simulations for two activated carbons, BPL carbon and a high surface area activated carbon made from Brazilian coconut shells (BCA), and make comparisons of the performance of each for storing and delivering methane or natural gas.

2 Gas storage system

A schematic of the gas storage vessel used in the simulations is shown in Figure 1. We consider a tank with a volume of approximately 23 L (ID = 0.2 m; L = 0.74 m). These dimensions have also been used in other studies (Chang and Talu, 1996; Mota et al., 1995). The vessel is packed with activated carbon and cycle steps are run to preset pressures. Discharge occurs at a constant flowrate of 6.2 L/min to a depletion pressure of 1.4 bar. The vessel is charged to 35 bar at a flowrate 20 times that of the discharge step.

Two types of activated carbon are used for process simulations. Physical properties are shown in Table 1. The natural gas feed is assumed to consist of methane with traces of ethane, propane, and butane. The gas composition and properties of each component are shown in Table 2.

3 Mathematical model

3.1 Multicomponent adsorption model

The proper description and prediction of adsorption equlibrium data are critical for the design and

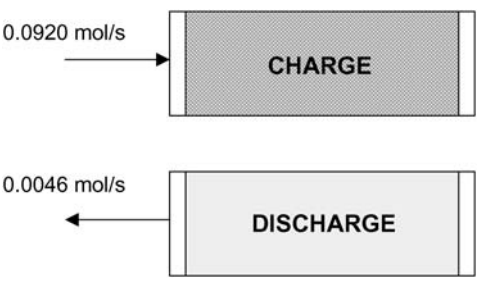

Fig. 1 Gas storage cycle steps

Table 1 Activated Carbon Properties

Property	BPL	BCA
ρ_b (kg/m^3)	460	300
ε'	0.70	0.85
R_p (m)	5.0×10^{-4}	5.0×10^{-4}
A_s (m^2/g)	1000	2100
C_{sol} (J/kg K)	1050	1300

simulation of a natural gas storage process. For this study, we have employed the group contribution theory of Walton et al. (2004). This theory has been shown to effectively predict the adsorption of alkanes, both pure-components and mixtures, on nanoporous carbons. The prediction of mixtures is inherent in this theory, so it is not necessary to use typical models such as the ideal adsorbed solution theory (Myers and Prausnitz, 1965). Temperature dependency is also built into this model. Therefore, the parameters given for alkanes adsorption on BPL carbon (Walton et al., 2004) and coconut shell carbon (Walton et al., 2005) are applicable to the entire operating range considered here.

Pure-component isotherms and model predictions for methane, ethane, and n-butane on both BPL and BCA carbon at 298 K are shown in Figure 2. Isotherms for these and other components and mixtures at different temperatures are given elsewhere (Walton et al., 2004, 2005). BCA carbon has higher capacities for butane than BPL carbon. However, the selectivities calculated using the group contribution theory for butane with respect to methane indicate that BPL carbon is more selective for butane than is BCA carbon. These selectivities are shown in Fig. 3. These differences should have an impact on gas storage cycle performance.

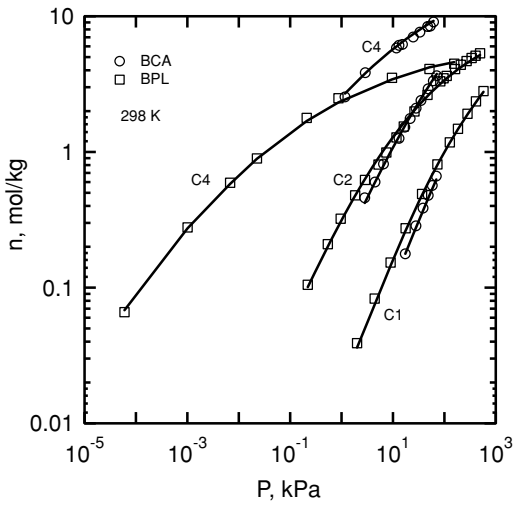

Fig. 2 Adsorption isotherms of methane, ethane, and butane on BPL and BCA carbons at 298 K. Symbols are experimental data, curves are group contribution theory Walton et al. (2004)

3.2 Modeling assumptions

The bed is initially loaded with pure methane at the depletion pressure. The charge/discharge steps occur from the same inlet/outlet in the gas storage cylinder (Fig. 1). We consider the pressure in the vessel to be spatially uniform and varying with time. There is no internal/external heating or cooling to compensate for the heat of adsorption. The intention here is to examine the extremes of the expected behavior. Thus, we model both adiabatic and isothermal cycles and determine bed profiles for both steps of the cycle.

Mass transfer is described by the linear driving force model. Fluid-phase concentrations are assumed to be much more dependent on pressure than temperature because of the large pressure swing between charge and discharge steps. This assumption is often used in pressure swing adsorption models in which the temperature swing is negligible compared to the change in pressure (Mahle et al., 1996). Heat capacities for all components in the feed are assigned constant gas-phase values, which are consistent with the thermodynamic path used to develop the energy balance (Walton et al., 2003). The heats of adsorption for each component are

Table 2 Adsorbate Properties

Parameter	Methane	Ethane	Propane	n-Butane
C°_{pg} (J/mol K) Poling (2001)	35.7	52.5	73.6	98.5
λ (kJ/mol) – BPL	15.5	22.7	29.3	36.0
λ (kJ/mol) – BCA	16.5	22.8	28.6	33.9
y_{feed}	0.88	0.08	0.03	0.01

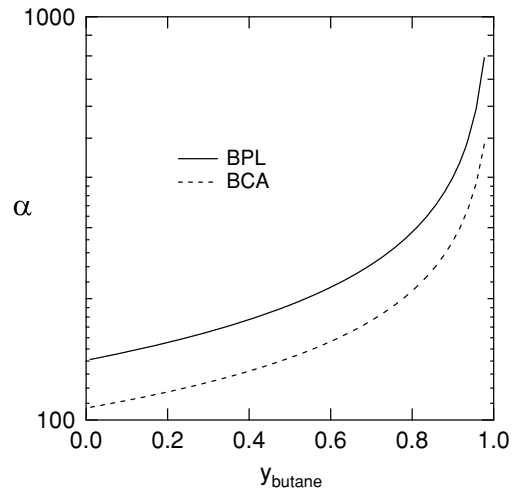

Fig. 3 Selectivities for butane with respect to methane calculated from group contribution theory

assumed to have constant values that were calculated as isosteric heats from the group contribution theory.

3.3 Material and energy balances

Overall material balance:

$$\rho_b \frac{\partial n}{\partial t} + \frac{\varepsilon'}{RT}\frac{dP}{dt} + \frac{P}{RT}\frac{\partial v}{\partial z} = 0 \tag{1}$$

Component material balance:

$$\rho_b \frac{\partial n_i}{\partial t} + \frac{\varepsilon'}{RT}\left[P\frac{\partial y_i}{\partial t} + y_i\frac{\partial P}{\partial t}\right] + \frac{1}{RT}\left[y_i P\frac{\partial v_i}{\partial z} + v_i P\frac{\partial y_i}{\partial z}\right] = 0 \tag{2}$$

Energy balance for fluid phase:

$$\rho_b \frac{\partial u_s}{\partial t} + \varepsilon'\frac{\partial (cu_f)}{\partial t} + \frac{\partial (vch_f)}{\partial z} = 0 \tag{3}$$

where internal energies and the enthalpy of the fluid phase are represented by

$$u_s = (C_{sol} + C^{\circ}_{pg} n)(T - T_{ref}) - \lambda n \tag{4}$$

$$u_f = h_f - P/c \tag{5}$$

$$h_f = C^{\circ}_{pg}(T - T_{ref}) \tag{6}$$

where

$$C^{\circ}_{pg} c = \sum_i C^{\circ}_{pgi} c_i \tag{7}$$

$$C^{\circ}_{pg} n = \sum_i C^{\circ}_{pgi} n_i \tag{8}$$

and

$$\lambda n = \sum_i \lambda_i n_i \tag{9}$$

The mass transfer rate is described by the LDF equation

$$\frac{\partial n_i}{\partial t} = k_{n_i}(n_i^* - n_i) \tag{10}$$

where the mass transfer coefficient is given by (Nakao and Suzuki, 1983)

$$k_{n_i} = \frac{15\psi D_{si}}{R_p^2} \tag{11}$$

where $\psi = 19/15$, and the diffusivity is represented by (Sladek et al., 1974)

$$D_{si}(m^2/s) = 1.6 \times 10^{-6} \exp(-0.45\ \lambda_{di}/RT) \tag{12}$$

where

$$\lambda_{di} = \lambda_i - RT \tag{13}$$

All spatial derivatives were written in backward difference form, resulting in a set of coupled first-order ordinary differential equations. The coupled system of equations was solved by Gear's method using LSODES, which includes a sparse matrix solver. The equations were solved for each step successively, so the bed profile at the end of the charge step provided the initial condition for solving the discharge step. Simulations were performed to 2500 cycles to approach the periodic condition.

4 Results and Discussion

4.1 Pure methane/BPL carbon

The mathematical model was solved for four different cases to examine gas storage behavior under various operating conditions. Figure 4 shows results for pure methane storage in BPL carbon under isothermal and adiabatic conditions. The bed profiles for the adiabatic

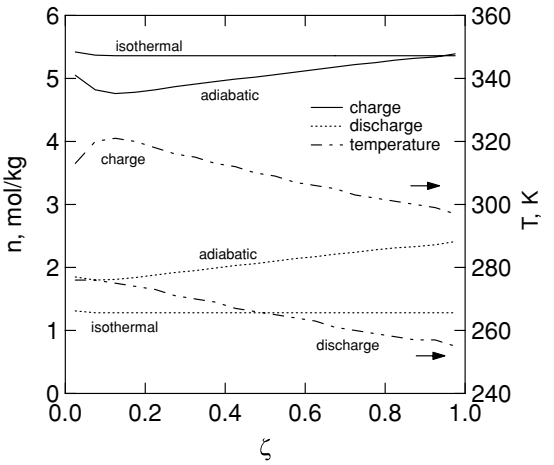

Fig. 4 Bed profiles for pure methane storage on BPL carbon. Adiabatic operation: 100 cycles; isothermal operation: any cycle

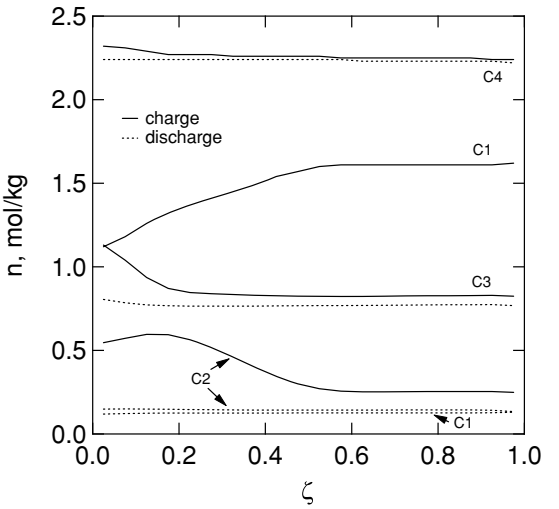

Fig. 5 Bed profiles for isothermal natural gas storage on BPL carbon after 2500 cycles have elapsed

case are given after 100 cycles have elapsed. The simulations were terminated at this point because the calculations showed that the system had approached the periodic condition, i.e., the changes in bed profiles from one cycle to the next were negligible. For the isothermal case, the bed profiles repeat after the first cycle.

A comparison of these two cases for pure methane shows that, as expected, nonisothermal effects decrease the storage capacity. The temperature profiles in Fig. 4 show that the bed is operating with a temperature swing of approximately 40 K between charge and discharge steps. It is also shown in Fig. 4 that less methane is stored and discharged for the adiabatic case than for the isothermal case. This is also evident in the time it takes for each step to complete; the isothermal charge step lasts for 12.6 min., while the time for the adiabatic charge step is 10.3 min. Because pure methane/isothermal is the ideal operating condition, we find from this case that approximately 4 mol/kg of methane is the maximum amount that can be stored using BPL carbon as the adsorbent.

4.2 Natural gas/BPL carbon

The bed profiles for natural gas on BPL carbon for charge and discharge steps under isothermal operation are shown in Fig. 5 for cycle 2500. It is apparent from the figure that butane accumulates in the bed after long times. This is true for propane as well. The accumulation of the heavier alkanes decreases the bed capacity such that less than half the amount of methane can be stored compared to the pure methane/isothermal case above.

The charge time further indicates the loss of capacity due to the build-up of butane. The bed is charged for 12.6 min for the first cycle but only 8 min for cycle 2500. There is also a significant decrease in the discharge time; cycle 1 discharges for 4.1 h while discharge for cycle 2500 lasts for 2.6 h.

Figure 6 shows long time behavior of natural gas storage cycles under adiabatic operation. The bed profiles in Fig. 6 show that the bed contains more butane and propane after long times than in the isothermal case. This occurs because the bed is operating in a subcooled condition with respect to the feed temperature, i.e., the bed cools more on discharge relative to the feed than it is heated during the feed step. We also find a slight decrease in the amount of methane stored for the adiabatic case, due to the greater adsorption of higher alkanes in the bed at colder temperatures. This is further demonstrated by the charge and discharge times; after 2500 cycles, the adiabatic process charges and discharges for 7.4 min and 2.4 h, respectively.

4.3 Natural gas/BCA carbon

Natural gas storage cycles were also simulated for an activated carbon made from Brazilian coconut shells. BCA carbon has high capacities for all of the alkanes, particularly butane, but it is actually less selective for

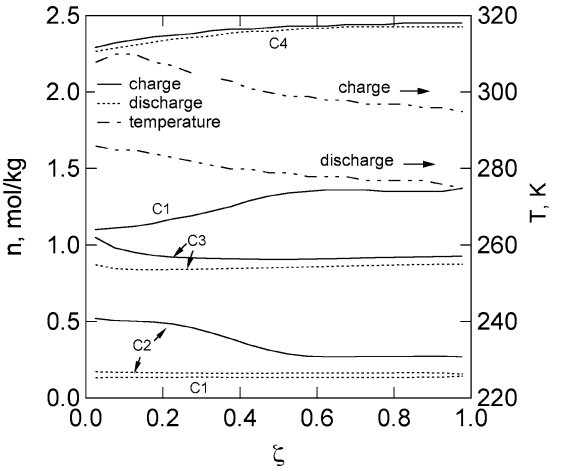

Fig. 6 Bed profiles for adiabatic natural gas storage on BPL carbon after 2500 cycles have elapsed

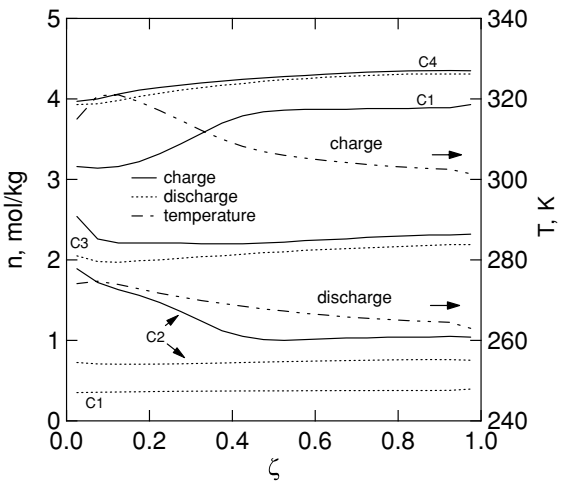

Fig. 7 Bed profiles for adiabatic natural gas storage on BCA carbon after 2500 cycles have elapsed

butane with respect to methane when compared to BPL carbon as shown in Fig. 3.

The high adsorption capacities translate to greater adsorption loadings during the charge step of the gas storage cycles. The bed profiles for natural gas are shown in Fig. 7 for cycle 2500 under adiabatic operation. BCA carbon has greater storage capacity for all of the alkanes compared to BPL. We find that butane accumulates in the bed at loadings greater than 4 mol/kg. Another striking difference between the two carbons is that BCA carbon stores more than twice as much methane as BPL, which is reflected by the longer charge and discharge times.

It was shown for BPL carbon in Figs. 4 and 6 that adiabatic cycles for pure methane and natural gas operate under subcooled conditions. For BCA carbon, the cycles also operate subcooled. Fig. 7 shows that the temperature at the end of the bed after cycle 2500 is 36 K less than the feed temperature. This is approximately 20 K cooler than the same cycle for BPL carbon. The heats of adsorption for both carbons are similar, so this large temperature difference can be attributed to the differences in volumetric heat capacities and actual adsorbed amounts as determined through the energy balance.

4.4 Dynamic efficiencies

A novel aspect of this study is that the mathematical model is solved for full process cycles. The results in Figs. 4–7 show degradation of storage performance due to nonisothermal effects and accumulation of heavy alkanes after long times. However, it is also important to understand the dynamic behavior of the storage cycles as the system approaches the periodic state.

Mota (1999) defined a dynamic efficiency, η_i, for measuring the net deliverable capacity of an ANG storage system. The efficiency is defined for each component by

$$\eta_i = \frac{Q_i/y_i}{Q_{1\,\mathrm{iso}}} \tag{14}$$

in which Q_i is the amount of species i delivered during discharge under dynamic conditions, y_i is the mole fraction of component i in the feed, and $Q_{1\,\mathrm{iso}}$ is the amount of pure methane delivered for an isothermal cycle. For the long-time periodic condition, components are discharged from the vessel in the same amounts as they are fed to the vessel during charging. Thus, the relative quantity of a component discharged will be proportional to its mole fraction in the feed for charging. Consequently, values of η_i will be the same for all components at the periodic condition and will relate the production of all components to that of pure methane delivered under isothermal conditions.

Figures 8 and 9 show efficiencies for the four components on BPL and BCA carbons, respectively, as a function of cycle number. Both plots are for adiabatic operation. The average bed temperature at the end of each cycle is also shown in the figures. For BPL carbon in Fig. 8, we find that the average bed temperature begins to decrease rapidly as ethane efficiency, η_2, in-

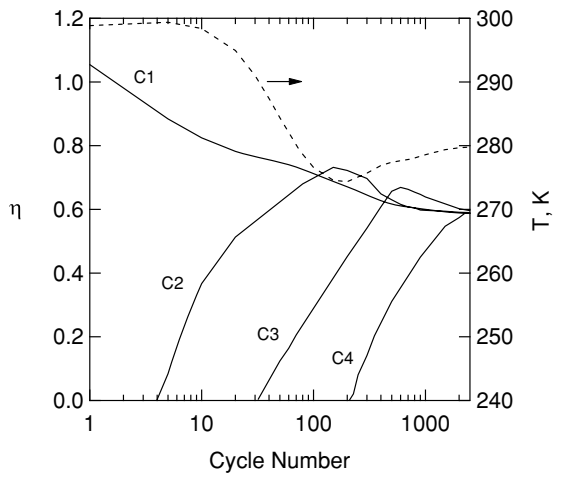

Fig. 8 Dynamic efficiencies of natural gas storage for BPL carbon as a function of cycle number. Temperature curve is average bed temperature at the end of each cycle

creases starting at the end of cycle 4. The temperature drop reaches a minimum when ethane efficiency is at a maximum at approximately cycle number 105. As η_2 increases, more ethane is being delivered and thus more is being desorbed. Thus, the temperature drop is directly related to adsorption and desorption of ethane. The same behavior is observed for BCA carbon in Fig. 9, but the average bed temperature drop is greater for this carbon than for BPL; this was also indicated by temperature profiles after long times in Figs. 6 and 7. For the long-time adiabatic behavior at the periodic condition, overall cyclic material and energy balances must be satisfied. Components fed to the storage vessel much be removed in the same amounts, and also the integral energy contents of the flows in and out of the vessel must match. The charge step will warm the bed due to the heat of adsorption, with the highest temperatures occurring at the feed end of the bed. Because of this, during discharge, the gas exiting the bed will initially be warm, but later it will be cooler as a result of having removed the warmth from the bed and supplying the energy for desorption. This leads to the development of a subcooled vessel after many cycles.

For natural gas under adiabatic conditions, we find that dynamic efficiencies converge to 0.60 and 0.63 for BPL and BCA carbons, respectively. In the work by Mota (1999), dynamic efficiencies were found to approach a value of approximately 0.3 for the carbon under consideration. The natural gas feed of that study contained traces of pentane and nitrogen, which lowers the efficiency. The profiles were solved only for the discharge step, and the charge step was always assumed to be isothermal.

Figure 10 provides a comparison of η_1 for both carbons. Efficiencies for methane are shown for pure methane feed/adiabatic operation and natural gas feed/isothermal operation. We find that for both carbons, η_1 is higher for the natural gas/isothermal process than for pure methane/adiabatic during the initial cycles. In fact, η_1 for pure methane/adiabatic on BCA carbon only exceeds η_1 for the natural gas/isothermal case after about 500 cycles. This shows

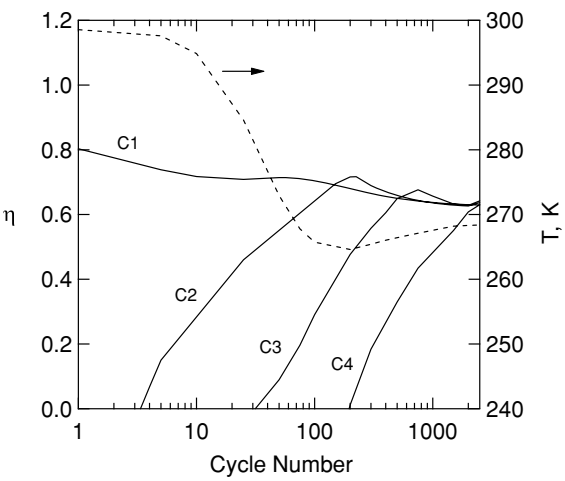

Fig. 9 Dynamic efficiencies of natural gas storage for BCA carbon as a function of cycle number. Temperature curve is average bed temperature at the end of each cycle

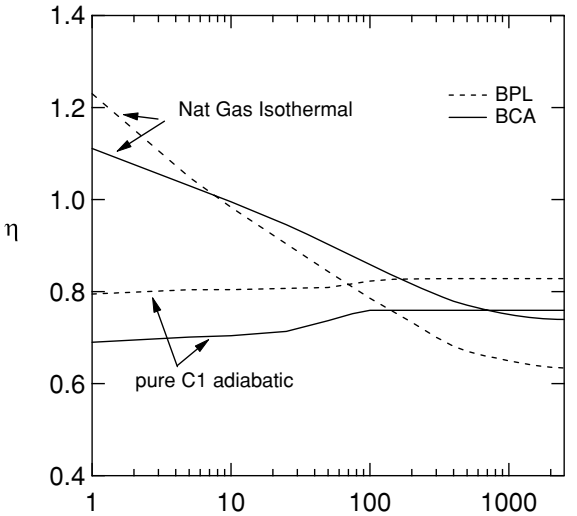

Fig. 10 Comparison of methane dynamic efficiencies, in natural gas or as pure methane, for BPL and BCA carbons

that for this case, nonisothermal effects are more detrimental to gas storage performance than the accumulation of heavy alkanes from natural gas. We also find, for BCA carbon, that discharge times are more than one hour longer for natural gas/isothermal than for pure methane/adiabatic after 50 cycles. The discharge time for pure methane does not exceed the natural gas discharge time until almost 500 cycles have elapsed.

There are a few factors that contribute to higher methane efficiencies for the natural gas/isothermal process. First, before the first storage cycle, the bed is at equilibrium with pure methane at the depletion pressure (1.4 bar). Thus, charging the system with pure methane will deliver almost the same amount during discharge. When charging with natural gas, the higher alkanes will selectively adsorb, and the methane initially present in the bed will be delivered on discharge along with the methane that was present in the natural gas feed. Therefore, more methane is delivered than is fed for the first several cycles.

The second factor contributing to greater initial methane efficiencies for natural gas/isothermal is found in Eq. (14), the definition of η. Because of this definition, η_1 will be greater than 1 if the amount of methane delivered under dynamic conditions is equal to the amount of pure methane delivered under isothermal conditions because the mole fraction of methane in the natural gas is less than 1 ($\eta_1 = 1.13$ for $y_1 = 0.88$).

5 Conclusions

A mathematical model has been developed and used to examine the influence of nonisothermal effects and accumulation of heavy alkanes on gas storage cycles. The model was solved for both the charge step and discharge step. This is the first study to obtain solutions for both cycle steps, allowing examination of bed profiles for temperature and all components in the process. Two activated carbons were considered and the model was solved for operational extremes, i.e., isothermal and adiabatic.

We find for both carbons that the adiabatic storage cycles operate under subcooled conditions. The bed will cool much more during the discharge step than it will heat up during the charge step relative to the feed temperature for the charge step. This behavior was seen for both pure methane and natural gas cycles. The average bed temperature for natural gas cycles was seen to drop dramatically as ethane begins to exit the bed with methane during discharge and reaches a minimum when ethane efficiency reaches a maximum.

Overall, natural gas/adiabatic cycles gave the worst storage performance and pure methane/isothermal resulted in the best performance, which is expected behavior based on previous work. However, we find that natural gas/isothermal cycles perform better than pure methane/adiabatic for the first 500 cycles for BCA carbon. The better performance can be seen in longer discharge times and greater methane efficiency. This result indicates that nonisothermal effects can be more detrimental to gas storage cycle performance than the presence of impurities in the feed.

In comparing the performance of the two carbons, we find that BCA carbon outperforms BPL carbon for natural gas storage, for both adiabatic and isothermal cases, but BPL performs better than BCA for storing pure methane. This is because BPL carbon is more selective for adsorbing the heavier alkanes than is BCA carbon.

Notation

c = gas-phase concentration, mol/m^3
C_{pa} = adsorbed-phase heat capacity, J/(mol K)
C°_{pg} = ideal gas heat capacity, J/(mol K)
C_{pl} = liquid heat capacity of water, J/(mol K)
C_{sol} = heat capacity of the solid, J/(kg K)
h_a = adsorbed-phase enthalpy, J/mol
h_f = fluid-phase enthalpy, J/mol
n = loading, mol/kg
P = pressure, Pa
R = ideal gas constant, J/(mol K)
T = temperature, K
u_s = internal energy of stationary phase, J/(kg K)

Greek Letters

ε' = total bed voidage
λ = isosteric heat of adsorption, J/mol
λ_d = differential heat of adsorption, J/mol
ρ_b = bulk density of the bed, kg/m^3
η = dynamic efficiency
ζ = dimensionless bed length, z/L

References

Biloé, S., V. Goetz, and A. Guillot, "Optimal Design of an Activated Carbon for an Adsorbed Natural Gas Storage System," *Carbon*, **40**, 1295–1308 (2002).

Biloé, S., V. Goetz, and S. Mauran, "Dynamic Discharge and Performance of a New Adsorbent for Natural Gas Storage," *AIChE J.*, **47**, 2819–2830 (2001).

Chang, K.J. and O. Talu, "Behavior and Performance of Adsorptive Natural Gas Storage Cylinders During Discharge," *Appl. Therm. Eng.*, **16**, 359–374 (1996).

Mahle, J.J., D.K. Friday, and M.D. LeVan, "Pressure Swing adsorption for Air Purification. 1. Temperature Cycling and Role of Weakly Adsorbed Carrier Gas," *Ind. Eng. Chem. Res.* **35**, 2342–2354 (1996).

Mota, J.P.B. "Impact of Gas Composition on Natural Gas Storage by Adsorption," *AIChE J.*, **45**, 986–996 (1999).

Mota, J.P.B., A.E. Rodrigues, E. Saatdjian, and D. Tondeur, "Charge Dynamics of a Methaned Adsorption Storage System: Intraparticle Diffusional Effects," *Adsorption*, **3** 117–125 (1997).

Mota, J.P.B., E. Saatdjian, D. Tondeur, and A.E. Rodrigues, "A Simulation Model of a High-Capacity Methane Adsorptive Storage System," *Adsorption*, **1**, 17–27 (1995).

Nakao, S. and M. Suzuki, "Mass Transfer Coefficient in Cyclic Adsorption and Desorption," *J. Chem. Eng. Jpn.* **16**, 114–119 (1983).

Poling, B.E., J.M. Prausnitz, and J.P. O'Connell, *The Properties of Gases and Liquids*, 5th ed., McGraw-Hill: New York, 2001.

Sladek, K.J., E.R. Gilliland, and R.F. Baddour, "Diffusion on Surfaces. II. Correlation of Diffusivities of Physically and Chemically Adsorbed Species," *Ind. Eng. Chem. Fund.* **13**(2), 100–105 (1974).

Walton, K.S., C.L. Cavalcante, and M.D. LeVan, "Adsorption Equilibrium of Alkanes on a High Surface Area Activated Carbon Prepared from Brazilian Coconut Shells," *Adsorption*, **11**, 107–111 (2005).

Walton, K.S. and M.D. LeVan, "Consistency of Energy and Material Balances for Bidisperse Particles in Fixed-Bed Adsorption and Related Applications," *Ind. Eng. Chem. Res.*, **42**, 6938–6948 (2003).

Walton, K.S., G. Pigorini, and M.D. LeVan, "Simple Group-Contribution Theory for Adsorption of Alkanes in Nanoporous Carbons," *Chem. Eng. Sci.*, **59**, 4425–4432 (2004).

Wegrzyn, J. and M. Gurevich, "Adsorbent Storage of Natural Gas," *Appl. Energy*, **55**, 71–83 (1996).

Myers, A.L. and J.M. Prausnitz, "Thermodynamics of Mixed-Gas Adsorption," *AIChE Journal*, **11**, 121–127 (1965).

Yang, R.T. *Adsorbents: Fundamentals and Applications*, John Wiley and Sons, Inc., New Jersey. Chapter 10, 2003.

Zhou, Z. "Thermal Analysis of Slow Discharge from a Pressurized Natural Gas Storage Tank," *Appl. Therm. Eng.*, **17**, 1099–1110 (1997).